Effect of a time-periodic axial shear flow upon the onset of Taylor vortices

H.-C. Hu and R. E. Kelly
Mechanical, Aerospace and Nuclear Engineering Department, University of California, Los Angeles, California 90024-1597
(Received 29 September 1994)

The onset of instability in the presence of an oscillatory axial flow between concentric rotating cylinders to both axisymmetric and nonaxisymmetric disturbances is investigated on a linear basis for a narrow-gap geometry. We consider two types of axial oscillation: one is due to an oscillatory pressure gradient, and the other is due to an oscillation of the inner cylinder. For small Reynolds numbers, the results are obtained for axisymmetric disturbances by expansion in terms of the amplitude of the oscillatory flow. For finite Reynolds numbers ($\mathrm{Re} \leq 100$), the governing equations are solved for general disturbances by a Galerkin expansion with time-dependent coefficients, and the stability boundaries of the system are determined by use of Floquet theory. The time-modulated axial flow, in general, stabilizes significantly axisymmetric disturbances except for some cases of counter-rotation with an oscillation of the inner cylinder. No subharmonic critical solutions appear for $\mathrm{Re} \leq 100$. For $\mathrm{Re} \leq 100$, axisymmetric disturbances are found to be more unstable than nonaxisymmetric ones when the outer cylinder is stationary, in contrast to the steady Poiseuille flow case for $\mathrm{Re} \gtrsim 30$. Nonaxisymmetric disturbances exhibit phase locking and jumps in the response frequency.

PACS number(s): 47.20.−k

I. INTRODUCTION

We consider an incompressible viscous fluid which is contained in the gap between two concentric cylinders that rotate about a common axis at constant but different angular velocities. Simultaneously, the inner cylinder oscillates axially or the fluid between the two cylinders is forced to oscillate by an oscillatory pressure gradient imposed in the axial direction. Our aim is to investigate the influence of the periodic motion upon the onset of axisymmetric and nonaxisymmetric Taylor vortices. The stability of a hydrodynamic system that has a time modulation can be affected significantly by suitable tuning of the basic nondimensional parameters. Many authors have investigated the effects of time modulation of the temperature at the boundaries in Rayleigh-Bénard convection or of the cylinders' rate of rotation for Taylor-Couette flow; see, e.g., the recent papers by Meyer, Cannel, and Ahlers [1] and by Donnelly [2], respectively. For Rayleigh-Bénard convection, the case when the fluid oscillates about a zero mean velocity and with constant wall temperature has been investigated only recently by Kelly and Hu [3,4]. In these papers, it is shown that nonplanar oscillatory shear can have a significant stabilizing effect, at least on a linear basis. This result caused us to initiate the present study because the predicted effect might be more easily observed in a laboratory experiment concerning centrifugal instability rather than for the case of thermal convection. For both situations, it is known that a steady shear corresponding to the type considered for the unsteady problem can have a stabilizing effect, and so stabilization would appear to be possible, at least in the quasisteady limit.

Time modulation of the angular velocities of the inner cylinder for Taylor-Couette flow leads to destabilization [5–8], in contrast to the stabilization that is predicted on a linear basis for thermal convection with time-modulated boundary temperatures, at least for nondimensional frequencies of order unity. However, theoretical results do not exist to our knowledge for the case of axial flow oscillations. Considerable work has been done for the case of a steady axial flow, and we now review this work because the results are relevant to the present problem in the quasisteady limit.

For axisymmetric disturbances, Chandrasekhar [9], Krueger and DiPrima [10], and DiPrima and Pridor [11] obtained numerical results for the effect of a steady axial Poiseuille flow with a fixed outer cylinder that indicate that the critical Taylor number increases initially with the Reynolds number. Nonaxisymmetric results were published by Chung and Astill [12], Takeuchi and Jankowski [13], Ng and Turner [14] and Babcock, Ahlers, and Cannel [15]. These authors found that the axisymmetric assumption is valid only for moderate values of Reynolds number (e.g., $\mathrm{Re} \lesssim 30$ for the case $\eta = 0.95$ when the outer cylinder is stationary, where η is the ratio of the radius of the inner cylinder to that of the outer one). For somewhat larger Reynolds numbers, nonaxisymmetric disturbances become critical, and the degree of stabilization is not as great as predicted for the axisymmetric case. Recently, Bühler and Polifke [16] and Lueptow, Docter, and Min [17] provided a stability diagram of the flow regimes in the Taylor-number–Reynolds-number plane.

In Sec. II we present the linearized governing equations with a narrow-gap approximation. In Sec. III we assume that the Reynolds number is very small, so that we can expand in terms of the Reynolds number and find explicitly the $O(\mathrm{Re}^2)$ correction to the critical Taylor number for axisymmetric disturbances. In Sec. IV we consider the Reynolds number to be finite. The Galerkin method is used to obtain a solution and leads to a set of first-order ordinary differential equations with time-periodic coefficients. The stability boundaries of this system are then determined by use of Floquet theory. Section V contains axisymmetric results for $\mu=1$, 0, and -1, and nonaxisymmetric results for $\mu=0$, where μ is the ratio of the angular velocity of the outer cylinder to that of the inner one. Section VI gives a summary.

II. THE GOVERNING EQUATIONS

We consider the stability problem of a viscous incompressible fluid between two infinite concentric cylinders that rotate about their common axis with constant angular velocities in the azimuthal (θ) direction when we force the fluid also to oscillate in the axial (z^*) direction. We define the radii (R_1,R_2) and the angular velocities (Ω_1,Ω_2) to be those of the inner and outer cylinders, respectively. In order to simplify this problem, we make the narrow-gap approximation, so that the gap width $d=R_2-R_1$ is small compared to their mean value $R_0=(R_2+R_1)/2$. If the dimensional frequency of the oscillatory flow W^* is ω^*, the velocity of the basic state is

$$U^*(t,\zeta)=\mathbf{i}_\theta V^*(\zeta)+\mathbf{i}_z W^*(t,\zeta) , \tag{1a}$$

where $\mathbf{i}_\theta$ and $\mathbf{i}_z$ are unit vectors and

$$\zeta=\frac{r^*-R_0}{d}, \quad -\tfrac{1}{2}\le\zeta\le\tfrac{1}{2} , \tag{1b}$$

and $t=\omega^* t^*$.

For the narrow-gap approximation, the steady velocity V^* is approximately equal to

$$V^*=\Omega_1 r^*[1-(1-\mu)(\zeta+\tfrac{1}{2})]+O(1-\eta) , \tag{2a}$$

where

$$\mu=\frac{\Omega_2}{\Omega_1} \quad\text{and}\quad \eta=\frac{R_1}{R_2}\cong 1 , \tag{2b}$$

There are two types of axial flows that we wish to consider. First, for pulsating Poiseuille flow due to a pressure gradient oscillation, $W^*(t,\zeta)$ is given by the solution of

$$2\beta^2\frac{\partial W^*}{\partial t}=-8W_0\cos t+\frac{\partial^2 W^*}{\partial\zeta^2} , \tag{3a}$$

$$W^*(t,-\tfrac{1}{2})=W^*(t,\tfrac{1}{2})=0 , \tag{3b}$$

where $\beta^2=\omega^* d^2/2\nu_0$ is a nondimensional frequency and $W_0=(\Delta p^*)_z d^2/\rho_0\nu_0 L$ is a characteristic velocity appropriate for the quasisteady limit ($\beta^2\to 0$). Here Δp^* denotes a pressure difference, ρ_0 is the density of fluid, ν_0 is the kinematic viscosity, and L is a characteristic length in the z^* direction. Let

$$W(t,\zeta)=\frac{W^*(t,\zeta)}{W_0}=\tfrac{1}{2}\phi_p(\zeta)e^{it}+\tfrac{1}{2}\tilde{\phi}_p(\zeta)e^{-it} , \tag{3c}$$

where a tilde denotes the complex conjugate; then

$$\phi_p(\zeta)=8\left\{-\frac{i}{2\beta^2}\left[\frac{e^{(1+i)\beta(1/2+\zeta)}-e^{-(1+i)\beta(1/2+\zeta)}}{e^{(1+i)\beta}-e^{-(1+i)\beta}}\right]-\frac{i}{2\beta^2}\left[\frac{e^{(1+i)\beta(1/2-\zeta)}-e^{-(1+i)\beta(1/2-\zeta)}}{e^{(1+i)\beta}-e^{-(1+i)\beta}}\right]+\frac{i}{2\beta^2}\right\} . \tag{3d}$$

Second, for flow due to an oscillation of the inner cylinder in the axial direction, $W^*(t,\zeta)$ is given by the solution of

$$2\beta^2\frac{\partial W^*}{\partial t}=\frac{\partial^2 W^*}{\partial\zeta^2} , \tag{4a}$$

$$W^*(t,-\tfrac{1}{2})=W_0\cos t \quad\text{and}\quad W^*(t,\tfrac{1}{2})=0 , \tag{4b}$$

where W_0 is the amplitude of the inner cylinder's velocity. Let

$$W(t,\zeta)=\frac{W^*(t,\zeta)}{W_0}=\tfrac{1}{2}\phi_c(\zeta)e^{it}+\tfrac{1}{2}\tilde{\phi}_c(\zeta)e^{-it} , \tag{4c}$$

then

$$\phi_c(\zeta)=\frac{e^{(1+i)\beta(1/2-\zeta)}-e^{-(1+i)\beta(1/2-\zeta)}}{e^{(1+i)\beta}-e^{-(1+i)\beta}} . \tag{4d}$$

We now perturb this basic state by a small disturbance which is assumed to vary periodically in the z^* direction and in the θ^* direction, so that the disturbance is expressed as

$$\begin{bmatrix} u_r^* \\ u_\theta^* \\ u_z^* \end{bmatrix}(t^*,r^*,\theta^*,z^*)=\begin{bmatrix} u^* \\ v^* \\ w^* \end{bmatrix}(t^*,r^*)e^{i(k^*z^*+n^*\theta^*)}+\text{c.c.} , \tag{5}$$

where k^* is the wave number, n^* is the azimuthal wave number, and c.c. denotes complex conjugate. We define the following nondimensional quantities: $z=z^*/d$, $k=k^*d$, $n=n^*$, $\theta=\theta^*$, $u=[u^*/R_1\Omega_1(2\Omega_1k^2d^2/\nu_0)]$, and $v=v^*/R_1\Omega_1$. After linearization of the Navier-Stokes equations, introduction of Eq. (5), and elimination of w^* and the perturbation pressure, we have the following characteristic value problem (see Krueger, Gross, and DiPrima [18]):

$$\left[2\beta^2\frac{\partial}{\partial t}+ik\,\mathrm{Re}W+inT_\eta\{1+\alpha(\zeta+\tfrac{1}{2})\}-\left[\frac{\partial^2}{\partial\zeta^2}-k^2\right]\right]\left[\frac{\partial^2}{\partial\zeta^2}-k^2\right]u-ik\,\mathrm{Re}\frac{\partial^2 W}{\partial\zeta^2}u=-[1+\alpha(\zeta+\tfrac{1}{2})]v , \tag{6a}$$

$$\left[2\beta^2\frac{\partial}{\partial t}+ik\,\mathrm{Re}W+inT_\eta\{1+\alpha(\zeta+\tfrac{1}{2})\}-\left[\frac{\partial^2}{\partial\zeta^2}-k^2\right]\right]v=k^2Tu , \tag{6b}$$

with the boundary conditions

$$u=\frac{\partial u}{\partial \zeta}=v=0 \quad \text{at } \zeta=\pm\tfrac{1}{2}\ , \tag{6c}$$

where the Reynolds number $\mathrm{Re}=W_0 d/\nu_0$, $\alpha=-(1-\mu)$, the Taylor number $T=-4\Omega_1 A d^4/\nu_0^2$, $A=-\Omega_1\eta^2[(1-\mu/\eta^2)/(1-\eta^2)]$ and $T_\eta=([(1-\eta^2)T/4(\eta^2-\mu)])^{1/2}$. We retain the curvature effect only in T and T_η.

III. THE ANALYSIS FOR SMALL REYNOLDS NUMBERS

In order to determine the effect of the oscillatory flow upon T_c for small Re, an expansion in powers of Re is used. For the axisymmetric case ($n=0$), the expansion goes as

$$u(t,\zeta)=u_0(\zeta)+\mathrm{Re}\,u_1(t,\zeta)+\mathrm{Re}^2 u_2(t,\zeta)+\cdots\ , \tag{7a}$$

$$v(t,\zeta)=v_0(\zeta)+\mathrm{Re}\,v_1(t,\zeta)+\mathrm{Re}^2 v_2(t,\zeta)+\cdots\ , \tag{7b}$$

$$T=T_c=T_{c,0}+\mathrm{Re}\,T_1+\mathrm{Re}^2 T_2+\cdots\ . \tag{7c}$$

Thus, as $\mathrm{Re}\to 0$, T_c is equal to the critical Taylor number for the case without an axial flow, namely, $T_{c,0}$. We wish to see how this critical value is affected by an imposed axial oscillation. It is argued that T_c cannot depend on the sign of Re because changing the sign of Re merely changes the phase of the oscillation by π, which should have no influence on the stability. It follows that all the odd coefficients in the Taylor number expansion, $T_1, T_3, \ldots$ are zero. The expansions (7a)–(7c) are substituted into Eqs. (6a) and (6b), and terms corresponding to the same power of Re are grouped together.

As $\mathrm{Re}\to 0$, we have the equations governing the classical Taylor problem, whereas the equations at $O(\mathrm{Re})$ involve nonhomogeneous terms that vary periodically with time. After separating out the time dependence, the resulting nonhomogeneous ordinary differential equations (ODE's) are solved by a shooting method appropriate for a two-point boundary value problem. The normalization used for the lowest order eigenfunctions was $(d^2u_0/d\zeta^2)=1$ at $\zeta=-\frac{1}{2}$. At $O(\mathrm{Re}^2)$, a mean nonhomogeneous term is produced via the Reynolds stress in addition to unsteady terms involving the harmonic of the forcing.

Due to the fact that the homogeneous part of the equation involving the steady nonhomogeneous term is the same as that arising at lowest order and so has a solution, a solution to the nonhomogeneous problem exists only if the Fredholm alternative is utilized. Its application involves use of the adjoint solution of the lowest order problem, which has been discussed by Roberts [19] and Chandrasekhar [20], and leads to a solvability condition involving T_2. The details of the analysis are not given here because they are rather similar to those presented by Kelly and Hu [3] for the case of shear modulated Rayleigh-Bénard convection. Values for T_2 will be given in Sec. V for axisymmetric disturbances. The main difference for the nonaxisymmetric case is that the lowest order solution is time dependent, which leads to a modification of the analysis described above.

IV. THE ANALYSIS FOR FINITE REYNOLDS NUMBERS

A. The numerical procedure — Galerkin method

Having shown how to solve the stability problem given by the axisymmetric version of Eqs. (6a) and (6b) for small values of the Reynolds number, we now discuss how to determine numerically the stability for finite values of the Reynolds number and for the nonaxisymmetric problem. Let the perturbation variables v and u be

$$v(t,\zeta)=\sum_{m=1}^{M} A_m(t)v_m(\zeta)\ , \tag{8a}$$

$$u(t,\zeta)=\sum_{m=1}^{M} B_m(t)u_m(\zeta)\ , \tag{8b}$$

where $A_m(t)$ and $B_m(t)$ are complex variables. The basis functions v_m are

$$v_m(\zeta)=\sqrt{2}\sin[m\pi(\zeta+\tfrac{1}{2})]\ , \tag{9a}$$

and u_m is beam function [22], namely

$$u_m(\zeta)=\frac{\sinh\left[\lambda_m\zeta+\dfrac{im\pi}{2}\right]}{\sinh[\frac{1}{2}(\lambda_m+im\pi)]}-\frac{\sin\left[\lambda_m\zeta+\dfrac{m\pi}{2}\right]}{\sin[\frac{1}{2}(\lambda_m+m\pi)]}\ , \tag{9b}$$

where λ_m is the positive roots of the equation

$$\tanh(\tfrac{1}{2}\lambda_m)=(-1)^m\tan(\tfrac{1}{2}\lambda_m)\ . \tag{10}$$

Both functions constitute complete orthonormal sets and are solutions of

$$D^2_{v_m}+m^2\pi^2_{v_m}=0,\quad v_m=0 \quad \text{at } \zeta=\pm\tfrac{1}{2}\ , \tag{11a}$$

$$D^4_{u_m}-\lambda_m^4 u_m=0,\quad u_m=Du_m=0 \quad \text{at } \zeta=\pm\tfrac{1}{2}\ , \tag{11b}$$

where $D=d/d\zeta$.

The series (8a) and (8b) is substituted into the linear perturbation equations (6a) and (6b), (6a) is multiplied by v_n and (6b) by u_n, and both equations are then integrated over range $(-\frac{1}{2},\frac{1}{2})$ to obtain a set of $2M$ complex equations:

$$2\beta^2\frac{dA_n}{dt}=\sum_{m=1}^{M}-(m^2\pi^2+k^2)\delta_{mn}A_m-ik\,\mathrm{Re}\sum_{m=1}^{M}\left[\int_{-1/2}^{1/2}Wv_m v_n\,d\zeta\right]A_m$$
$$-inT_\eta\sum_{m=1}^{M}\left[\int_{-1/2}^{1/2}\{1+\alpha(\zeta+\tfrac{1}{2})\}v_m v_n\,d\zeta\right]A_m+k^2T\sum_{m=1}^{M}\left[\int_{-1/2}^{1/2}u_m v_n\,d\zeta\right]B_m\ , \tag{12a}$$

$$2\beta^2 \sum_{m=1}^{M} \left[\int_{-1/2}^{1/2} u_n D^2 u_m d\zeta - k^2 \delta_{mn} \right] \frac{dB_m}{dt}$$
$$= -\sum_{m=1}^{M} \left[\int_{-1/2}^{1/2} \{1+\alpha(\zeta+\tfrac{1}{2})\} v_m u_n d\zeta \right] A_m + \sum_{m=1}^{M} \left[(\lambda_m^4 + k^4)\delta_{mn} - 2k^2 \int_{-1/2}^{1/2} u_n D^2 u_m d\zeta \right] B_m$$
$$- ik\mathrm{Re} \sum_{m=1}^{M} \left[\int_{-1/2}^{1/2} \{ W u_n (D^2 - k^2) u_m - \frac{\partial^2 W}{\partial \zeta^2} u_m u_n \} d\zeta \right] B_m$$
$$- inT_\eta \sum_{m=1}^{M} \left[\int_{-1/2}^{1/2} \{ [1+\alpha(\zeta+\tfrac{1}{2})] u_n (D^2-k^2) u_m \} d\zeta \right] B_m , \tag{12b}$$

where δ_{mn} is the Kronecker delta. Define

$$\Xi_{nm} = \sum_{m=1}^{M} \left[\int_{-1/2}^{1/2} u_n D^2 u_m d\zeta - k^2 \delta_{mn} \right] ,$$
$$n = 1,2,\ldots,M . \tag{13}$$

For computational purposes it is convenient to rearrange (12a) and (12b). First, we multiply (12b) by the inverse of the matrix made up of the elements (13). Now introduce the notation

$$Y_1 = A_1, \quad Y_2 = A_2, \ldots, Y_M = A_M , \tag{14a}$$

$$Y_{M+1} = B_1, \quad Y_{M+2} = B_2, \ldots, Y_{2M} = B_M . \tag{14b}$$

Equations (12a) and (12b) can then be written in the form

$$\frac{dY_i}{dt} = G_{ij}(t) Y_j, \quad i,j = 1,2,,\ldots,2M , \tag{15}$$

where the matrix $G_{ij}(t)$ is composed of the coefficients in (12a) and (12b) and is periodic in t with period 2π.

B. The application of Floquet theory

Our problem is now reduced to analyzing the stability of a set of complex first-order periodic ordinary differential equations. This will be accomplished using classical Floquet theory [23] and numerical integration. Let $\mathbf{X}$ be a $2M \times 2M$ fundamental matrix for Eq. (15). We then have

$$\frac{d\mathbf{X}}{dt} = \mathbf{G}\mathbf{X}, \quad \mathbf{X}(0) = \mathbf{I} , \tag{16}$$

where $\mathbf{I}$ is the $2M \times 2M$ identity matrix. There exists a constant nonsingular matrix $\mathbf{R}$ such that

$$\mathbf{X}(t+2\pi) = \mathbf{X}(t)\mathbf{R} . \tag{17}$$

Moreover, let

$$\mathbf{R} = e^{2\pi \mathbf{C}} , \tag{18}$$

where $\mathbf{C}$ is a constant matrix. The matrix $\mathbf{X}$ may be represented as

$$\mathbf{X}(t) = \mathbf{P}(t) e^{t\mathbf{C}}, \quad \mathbf{X}(0) = \mathbf{P}(0) = \mathbf{I} , \tag{19}$$

where $\mathbf{P}(t)$ is a 2π-periodic matrix. We integrate Eq. (16) over one period to find $\mathbf{X}(2\pi)$ and obtain

$$\mathbf{X}(2\pi) = \mathbf{P}(2\pi) e^{2\pi\mathbf{C}} = \mathbf{P}(0) e^{2\pi\mathbf{C}} = \mathbf{I} e^{2\pi\mathbf{C}} . \tag{20}$$

Hence

$$\gamma_j = e^{2\pi\sigma_j}, \quad j = 1,2,\ldots,2M , \tag{21}$$

where γ_j is the characteristic multiplier of $\mathbf{X}(2\pi)$, and σ_j the characteristic exponent (or Floquet exponent) of $\mathbf{C}$. The imaginary parts of the characteristic exponents $\mathcal{I}(\sigma_j)$ are not determined uniquely. We can add $\pm l$, $l = 0,1,2,\ldots$ to them. The values of the real part of the characteristic exponent $\mathcal{R}(\sigma_j)$ determine the stability of the system. Order the real part of the characteristic exponents so that $\mathcal{R}(\sigma_1)$ has the greatest value; the system is then stable if $\mathcal{R}(\sigma_1) < 0$, while $\mathcal{R}(\sigma_1) = 0$ defines a stability boundary and corresponds to one periodic solution. At the stability boundary, if the principal value of the imaginary part of σ_1, $\mathcal{I}(\sigma_1)$, is zero, then $\gamma_1 = 1$ and the disturbance is synchronous with the imposed oscillation, whereas if $\mathcal{I}(\sigma_1) = \pm\frac{1}{2}$, then $\gamma_1 = -1$ and so the disturbance has a frequency equal to half that of the imposed oscillation, corresponding to a subharmonic response of order $\frac{1}{2}$.

Our numerical technique consists of a forward integration scheme and an eigenvalue finder. Usually the Runge-Kutta integration method is employed to obtain $\mathbf{X}(2\pi)$. However, the system becomes stiff if the Reynolds number Re is very large and the frequency β is very small, or if the cylinders counter-rotate ($\mu < 0$). We then need to use Gear's backward differentiation formulas (BDF's) [21] to complete the integration. All the numerical work is done in double precision, and $M = 7$ is sufficient for the purpose of numerical convergence because the difference in the results between $M = 7$ and 9 was found to be much less than 1% for high or low frequency β and different μ's.

V. RESULTS AND DISCUSSION

A. Axisymmetric disturbances

We have considered the stability of Taylor vortex flow with different ratios of angular velocities $\mu = 1$, 0, and -1. Although axisymmetric instabilities are less likely for $\mu = \pm 1$ than for $\mu = 0$ based on steady flow results (cf. Busse [24] and Krueger and DiPrima [10]), we include these results in order to provide some comparison to the

$\mu=0$ case. In order to test our results for the limiting case $\beta \rightarrow 0$, we compare our quasi-steady-state results for an oscillating pressure gradient with the axisymmetric steady flow results of Krueger and DiPrima [10] and DiPrima and Pridor [11]. However, we note that our Reynolds number definition is different from that of Krueger and DiPrima. Krueger and DiPrima used the cross-sectional average of the axial flow as a reference, whereas we use the maximum velocity. As a result, Krueger and DiPrima's Reynolds number is $\frac{2}{3}$ of our Reynolds number Re.

Our axisymmetric results for $\mu=0$ will be limited initially to values of $\mathrm{Re} \leq 30$ because the assumption of axisymmetric flow would seem to be dubious for larger values based on the steady flow results [13]. For these values of Re as well as larger values that we have tested, only synchronous solutions have been obtained for axisymmetric disturbances. The first case that we consider has $\mathrm{Re}=30$ and corresponds to an oscillating pressure gradient. Results are presented in Fig. 1 for $\mu=0$ and -1; the results for $\mu=1$ for axisymmetric flow nearly coincide with those for $\mu=0$. Maximum stabilization occurs as $\beta \rightarrow 0$ and the amount of stabilization decreases continuously as β increases. For high frequencies, $\beta>6$, there is almost no stabilization, due to the fact that the oscillatory shear layer is very thin compared to the gap width between the cylinders. But at low frequency $\beta<1$, shear exists throughout the gap. In this case, the stabilizing effect in the quasisteady state is almost the same as one half that corresponding to steady flow with the factor of $\frac{1}{2}$, due to the fact that the stabilizing (or destabilizing) mechanism in our case involves the mean-squared value of the oscillatory shear. The increase of the critical Taylor number in the quasisteady state is in good agreement with one half that of Krueger and DiPrima [10] and DiPrima and Pridor [11] for $\mu=0$ and 1. For $\mu=-1$, however, Krueger and DiPrima's results are inaccurate because they only used three expansion terms in their calculation. We recalculated the case for $\mathrm{Re}=30$ and found $T_c=22\,429$ and $T_{c,0}=18\,667$. We see that $(T_c-T_{c,0})/T_{c,0}$ in the quasisteady limit is almost the same as one half that of the steady solution. However, the quasisteady result needs to be used with caution, due to the fact that special analysis is needed at those instants when the shear is zero. The situation is similar to that investigated by Barenghi and Jones [5] for the case of inner cylinder modulation of tangential velocity for Taylor-Couette flow; see also Hall [25] for a discussion of the effects of nonplanar flow oscillations on the onset of thermal convection in this limit.

The critical Taylor number and wave number for a steady axial flow induced by motion of the inner cylinder are shown in Fig. 2. The critical Taylor numbers increase monotonically with the Reynolds numbers, except for $\mu=-1$ for which slight destabilization first occurs. The maximum destabilization occurs at $\mathrm{Re} \cong 35$ for $\mu=-1$, and stabilization occurs for $\mathrm{Re} \gtrsim 55$. The critical wave numbers decrease monotonically with the Reynolds numbers for all three rotation ratios.

Returning now to the oscillatory flow case, let us compare some results of the small Reynolds number analysis with those from the finite Reynolds number analysis for $\mu=1$, 0, and -1. Figure 3 and 4 show the results for the case of a pressure gradient oscillation and Figs. 5 and 6 show the results for the case of an inner cylinder axial oscillation. In the finite Reynolds number analysis, $(T_c-T_{c,0})/\mathrm{Re}^2 T_{c,0}$ is analogous to the term $T_2/T_{c,0}$ in the small Reynolds number analysis. We first let $\mu=1$ so $T_{c,0}=1707.8$ in Fig. 3. The maximum stabilization occurs in the quasisteady limit regardless of whether the Reynolds number is small or large. The amount of the stabilizing effect decreases continuously as β increases. This figure also shows that the results for $T_2/T_{c,0}$ are almost the same as those for $(T_c-T_{c,0})/\mathrm{Re}^2 T_{c,0}$ as determined by the finite Reynolds number analysis of Sec. IV, at least for Reynolds numbers up to 30. In order to ex-

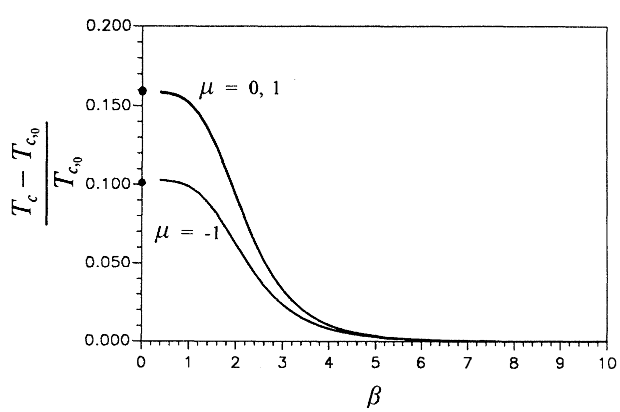

FIG. 1. The ratio of the increase in the amount of stabilization due to an oscillatory pressure gradient to the critical Taylor number without axial shear as a function of the nondimensional frequency β:Re$=30$; $\mu=0$, and $T_{c,0}=3390$; $\mu=1$ and $T_{c,0}=1707.8$; and $\mu=-1$ and $T_{c,0}=18\,667$; ●: for steady Poiseuille flow at Re$=30$ [10,11].

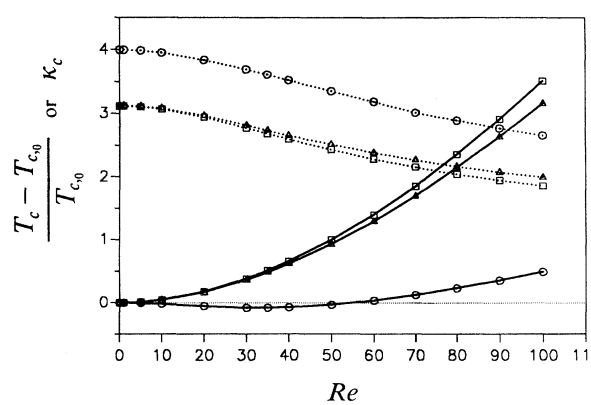

FIG. 2. Solid line: the ratio of the increase in the amount of stabilization due to a steady axial flow induced by the inner cylinder to the critical Taylor number without axial shear as a function of the Reynolds number. Dotted line: the critical wave number as a function of the Reynolds number: □ for $\mu=1$ and $T_{c,0}=1707.8$; △ for $\mu=0$ and $T_{c,0}=3390$; ○ for $\mu=-1$ and $T_{c,0}=18\,667$.

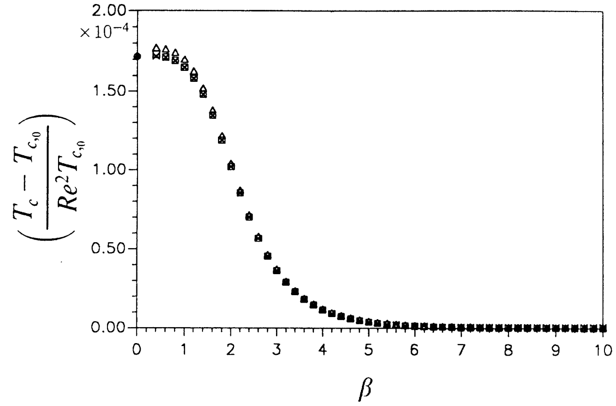

FIG. 3. The amount of stabilization for different Reynolds numbers due to an oscillatory pressure gradient as a function of the nondimensional frequency β: $\mu=1$; □: $T_2/T_{c,0}$ for Re $\ll 1$; ×: $(T_c - T_{c,0})/\mathrm{Re}^2 T_{c,0}$ for Re=1; △: $(T_c - T_{c,0})/\mathrm{Re}^2 T_{c,0}$ for Re=30; ●: the steady Poiseuille flow result from Datta [26].

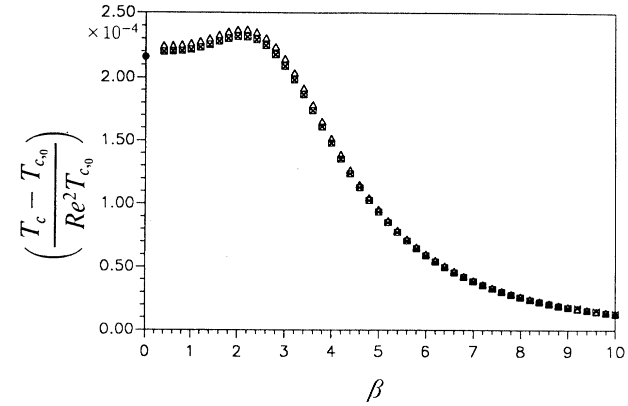

FIG. 5. The amount of stabilization for different Reynolds numbers due to an oscillation of the inner cylinder as a function of the nondimensional frequency β: $\mu=1$; □: $T_2/T_{c,0}$) for Re $\ll 1$; ×: $(T_c - T_{c,0}/\mathrm{Re}^2 T_{c,0}$ for Re=1; △: $(T_c - T_{c,0})/\mathrm{Re}^2 T_{c,0}$ for Re=30; ●: the steady result at Re=30.

plain this phenomena, we examined the steady flow results of Datta [26], who derived a formula for the critical Taylor number as $k_c = 3.12$ and $\mathrm{Re} \to 0$ under the conditions of steady axial Poiseuille flow and corotating cylinders ($\mu=1$). We modified his formula to suit our problem and obtained the following expression:

$$T_c = 1707.8 + \frac{1.32}{2}\left[\frac{4}{9}\mathrm{Re}^2\right] . \tag{22}$$

The value of $(T_c - 1707.8)/\mathrm{Re}^2 1707.8 = 0.000\,171\,76$ confirms our calculation for the quasisteady state. Datta's formula can be used to predict the critical Taylor number when Re is as large as 30, the error for Re=30 being about 5%. It is thus not surprising that our small Reynolds number analysis is also accurate for Reynolds number up to 30 in the quasisteady limit; the results shown in Fig. 3 indicate that the agreement is not dependent on the value of β. In Fig. 4, we let $\mu=0$, $T_{c,0}=3390$ and $\mu=-1$, $T_{c,0}=18\,667$. Both figures show properties similar to those shown in Fig. 3.

Next we show some results for the case when the inner cylinder undergoes an axial oscillation. In Fig. 5, we let $\mu=1$ and $T_{c,0}=1707.8$. We note that this figure shows a different trend compared to Figs. 3 and 4 as β changes. Although the amount of stabilization still decreases with β for very large values of β, the maximum amount of stabilization no longer occurs as $\beta \to 0$. The maximum increase of the Taylor number occurs at approximately $\beta \cong 2.2$. The curves of the small and finite Reynolds number analyses are again almost the same for Reynolds numbers up to 30. The result of the quasisteady limit again agrees with that for steady axial flow induced by

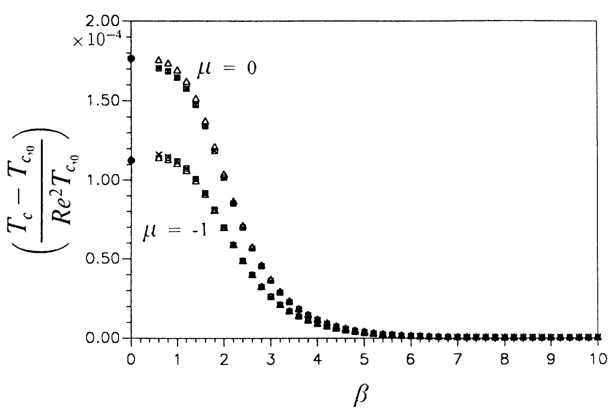

FIG. 4. The amount of stabilization for different Reynolds numbers due to an oscillatory pressure gradient as a function of the nondimensional frequency β: $\mu=0$, -1; □: $T_2/T_{c,0}$ for Re $\ll 1$; ×: $(T_c - T_{c,0})/\mathrm{Re}^2 T_{c,0}$ for Re=1; △: $(T_c - T_{c,0})/\mathrm{Re}^2 T_{c,0}$ for Re=30; ●: the steady result at Re=30.

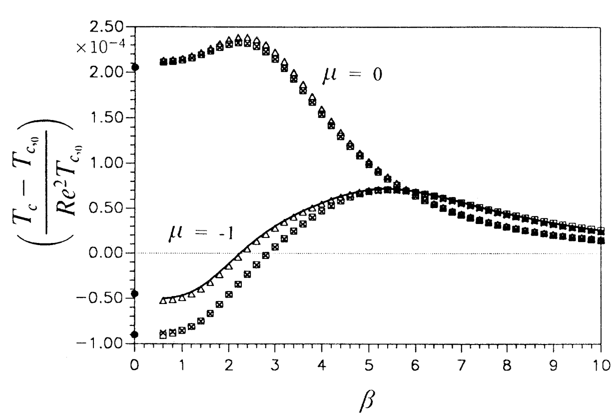

FIG. 6. The amount of stabilization for different Reynolds numbers due to an oscillation of the inner cylinder as a function of the nondimensional frequency β: $\mu=0$, -1; □: $T_2/T_{c,0}$ for Re $\ll 1$; ×: $(T_c - T_{c,0})/\mathrm{Re}^2 T_{c,0}$ for Re=1; △: $(T_c - T_{c,0})/\mathrm{Re}^2 T_{c,0}$ for Re=30; solid line $(T - T_{c,0})/\mathrm{Re}^2 T_{c,0}$ at $\kappa = 3.999$ for Re=30; ●: the steady result at Re=30 and 1.

motion of the inner cylinder for Re=30. In Fig. 6, $T_{c,0}=3390$ for $\mu=0$, whereas $T_{c,0}=18\,667$ for $\mu=-1$. For $\mu=0$, we have the same conclusions as for Fig. 5. For $\mu=-1$, we see that destabilization now occurs for $\beta<3$ and that the maximum amount of destabilization occurs in the quasisteady limit. From Fig. 2 we know that an increase of the Reynolds number will lead to stabilization eventually. However, we do not know whether or not the maximum increase of critical Taylor number will occur in the quasisteady limit or at some finite β; this needs further study. We indicate by a solid line the results at a fixed wave number, $\kappa=3.999$, equal to the critical wave number without an axial shear flow. It appears that the critical Taylor number is not affected too much by change in the critical wave number for different imposed frequencies β.

Next we will show some critical values of Taylor numbers and wave numbers for different Reynolds numbers with $\mu=0$. We examine the cases of $\beta=1$ and 2.5. We see in Fig. 7 that the critical Taylor number increases as the Reynolds number increases for both cases. In Fig. 8, we see that the critical wave number increases slightly as the Reynolds number increases for the case of a pressure gradient oscillation, but that the critical wave number decreases significantly as the Reynolds number increases for the case of an oscillation of the inner cylinder. Figure 8 also shows that the critical wave numbers for both cases are almost the same when Re $\lesssim 30$. For the case of oscillatory Couette flow, the characteristic velocity W_0 is equal to $(\delta^*\omega^*)$, where δ^* is a characteristic displacement of the wall. It follows that $\delta^*/d=\mathrm{Re}/2\beta^2$ so that $\delta^*\gg d$ for either large Re or small β. For $\beta=2.2$, $\delta^*/d\cong 0.103\mathrm{Re}$, so that the effect can be realized most easily for thin layers, which, of course, are typical of lubrication problems.

It should again be emphasized that the prediction of an increase of critical Taylor number is limited by the assumption that the disturbances are axisymmetric. For the case of a steady axial Poiseuille flow, axisymmetric disturbances are more unstable up to Re=30 when $\mu=0$, and so next we investigate if the same is true for unsteady flow.

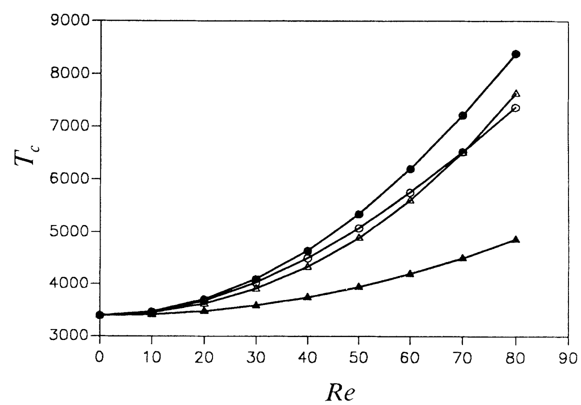

FIG. 7. The critical Taylor number as a function of the Reynolds number. $\mu=0$; ○: $\beta=1$; and ●: $\beta=2.5$ for the oscillation of the inner cylinder. △: $\beta=1$ and ▲: $\beta=2.5$ for the oscillation of a pressure gradient.

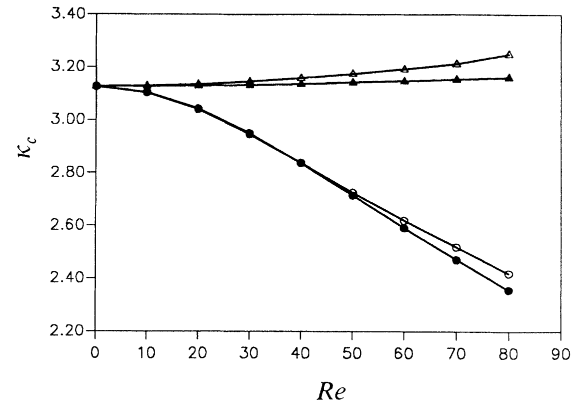

FIG. 8. The critical wave number as a function of the Reynolds number. $\mu=0$; ○: $\beta=1$; and ●: $\beta=2.5$ for the oscillation of the inner cylinder. △: $\beta=1$ and ▲: $\beta=2.5$ for the oscillation of a pressure gradient.

B. Nonaxisymmetric disturbances

In this section we discuss briefly some results for nonaxisymmetric disturbances ($n\neq 0$) for the case of oscillating Poiseuille flow. We choose $\eta=0.95$ for the following calculations in order to satisfy the narrow-gap assumption. Besides the critical Taylor number and corresponding wave number, we wish to describe the time-dependent behavior of the disturbances, which, as we will show, is not necessarily synchronous with the forcing for nonaxisymmetric disturbances. For this purpose, we introduce a quantity called the characteristic response frequency of the disturbance that depends linearly upon $\mathcal{I}(\sigma_1)+l$, where l is, as noted after Eq. (21), an arbitrary integer as far as the Floquet exponent is concerned. We will fix l by comparison with the unmodulated case; say then that $\mathcal{I}(\hat{\sigma}_1)$ is the resulting value of the above quantity. We now define the characteristic response frequency of the disturbance as $f_r=2\beta^2\mathcal{I}(\hat{\sigma}_1)$. By use of this frequency, we are essentially using the diffusive time scale

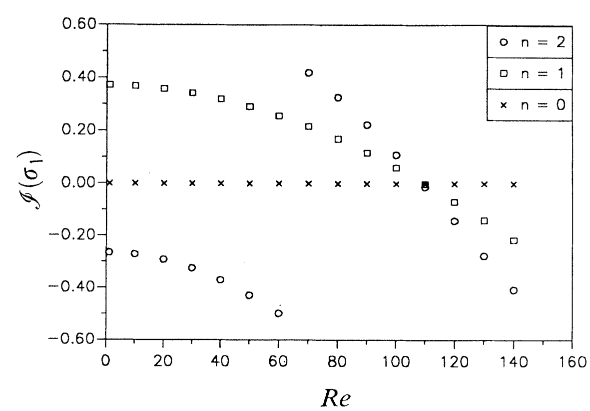

FIG. 9. The imaginary part of the Floquet exponent as a function of the Reynolds number for different azimuthal wave numbers: $\mu=0$, $\beta=2$, and $\eta=0.95$ for $n=0$, 1, and 2.

(d^2/ν_0) instead of $(1/\omega^*)$, which is desirable when making the comparison to the unmodulated case. With this diffusive time scale, the forcing frequency becomes $f_f=2\beta^2$.

The numerical results for $\mathcal{J}(\sigma_1)$ are shown in Fig. 9. For the axisymmetric case, $\mathcal{J}(\sigma_1)=0$, because a synchronous response occurs, and so we take $l=0$. For $n=1$ and 2, however, $\mathcal{J}(\sigma_1)\neq 0$ and is dependent upon both n and Re. For $\mathcal{J}(\sigma_1)\neq 0$ or $\pm\frac{1}{2}$, the disturbance (for a neutrally stable case) is quasiperiodic, with f_f and f_r being the two frequencies. We first want to relate our results for the case Re$\rightarrow 0$ to the results of Krueger, Gross, and DiPrima [18] for nonaxisymmetric Taylor vortices without axial flow. If we denote the frequency of the most unstable disturbance found by Krueger, Gross, and DiPrima as $f_{0,n}$, then from [18] $f_{0,1}=-4.8534$ and $f_{0,2}=-9.7661$ for a value of $\eta=0.952\,381$. If we take $l=-1$, then, as Re$\rightarrow 0$, our results, from Fig. 9 and using $\mathcal{J}(\hat{\sigma}_1)=\mathcal{J}(\sigma_1)-1$, are $f_{r,1}=-5.0246$ and $f_{r,2}=-10.1232$ for $\beta=2$. The agreement is quite reasonable, and indicates that we have chosen the correct value of l.

For Re slightly greater than 60 in Fig. 9, a jump in $\mathcal{J}(\sigma_1)$ from $-\frac{1}{2}$ to $\frac{1}{2}$ occurs corresponding to a jump in $\mathcal{J}(\hat{\sigma}_1)$ from $-\frac{3}{2}$ to $-\frac{1}{2}$. The characteristic response frequency seems to undergo a sudden adjustment once it goes too far below the unmodulated natural frequency to a frequency somewhat above $f_{0,2}$ (i.e., from $f_{r,2}\cong -12$ to $f_{r,2}\cong -4$). With further increase in Re, $f_{r,2}$ again begins to become more negative, becomes equal to f_f at Re$\cong$110, then declines further until presumably a second jump occurs at a still higher value of Re. The result for $f_{r,1}$ shows a steady decrease, but presumably a jump also occurs in it for a still higher value of Re than shown.

The jumps shown in Fig. 9 for a fixed value of f_f as Re increases also occurs for a fixed value of Re as f_f increases, as shown in Fig. 10 for $n=2$, $\mu=0$, and Re$=0.1$. For large forcing frequencies ($f_f \gtrsim 20$), $f_{r,2}$ is equal to $f_{0,2}$, namely -10.1232. For such high values of β, the effect of modulation can be expected to be slight, and one should expect $f_{r,2}\cong f_{0,2}$. The interesting aspect is that the change to $f_{r,2}$ occurs suddenly at a certain value of β, rather than gradually over a range of β. The jump from $f_{r,2}\cong -10.12$ to 10.12 as f_f decreases below $2f_{0,2}$, so that the response is a subharmonic of order $\frac{1}{2}$ with regard to the forcing. The change in sign of $f_{r,2}$ means that the helical nature of the disturbance changes direction. For further decrease in f_f, the disturbance becomes synchronous with the forcing when $f_f=f_{0,2}$ and then becomes negative again until another jump occurs to a positive value of $f_{r,2}$. Notice that the response is always synchronous when $f_f=f_{0,2}/m$, $m=1,2,3.\ldots$ By connecting the values of $f_{r,2}$ at which the jumps occur for $f_{r,2}>0$, and also for $f_{r,2}<0$, an envelope of possible values for $f_{r,2}$ is defined. Within this envelope, quasiperiodic behavior predominates. As $f_f\rightarrow 0$, the extent of the envelope becomes small, suggesting synchronous motion in the quasisteady limit. As mentioned previously, however, a separate analysis is required in this limit. The jumps occur when $f_f=2f_{0,2}/(2N+1), N=0,1,2,3,\ldots.$ The response frequency always jumps to a value corresponding to a subharmonic of order $\frac{1}{2}$ with respect to the forcing. In Fig. 11, the slope of the response frequency (f_r) with respect to the forcing frequency (f_f) is constant, $\Delta f_r/\Delta f_f=N$, $N=0,1,2,\ldots.$ There are different stages corresponding to different forcing frequency regions. When the forcing frequency is small, the slope is large but the band becomes narrow. For large forcing frequencies ($f_f\gtrsim 20$), the slope is zero. This means that the response frequency is equal to the most-amplified frequency $f_{0,2}$ for such a high forcing frequency. The reason is the same as we have mentioned in regard to Fig. 10.

Ho and Huang [27] observed somewhat similar jumps in the response frequency in experiments concerning a temporally forced mixing layer when the forcing frequency was too far away from the most probable natural frequency. In that case, however, the jump occurred so that the most probable natural frequency was obtained after the jump. In the interval between jumps, the response frequency was constant and equal to a subharmonic of order N with regard to the forcing frequency. In these

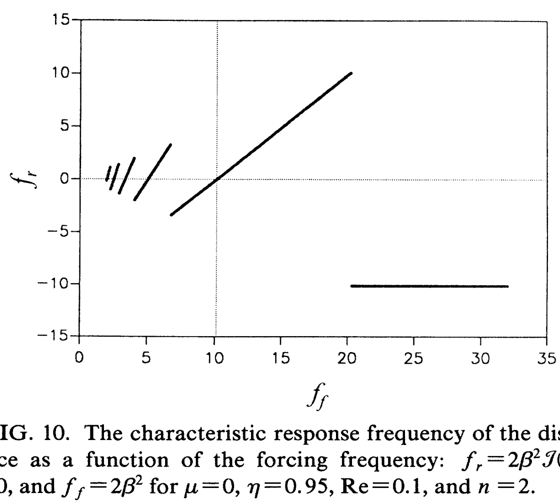

FIG. 10. The characteristic response frequency of the disturbance as a function of the forcing frequency: $f_r=2\beta^2\mathcal{J}(\hat{\sigma}_1)$, $l=0$, and $f_f=2\beta^2$ for $\mu=0$, $\eta=0.95$, Re$=0.1$, and $n=2$.

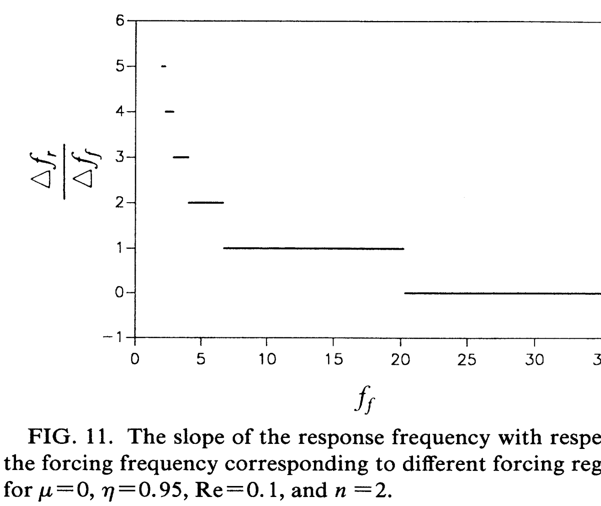

FIG. 11. The slope of the response frequency with respect to the forcing frequency corresponding to different forcing regimes for $\mu=0$, $\eta=0.95$, Re$=0.1$, and $n=2$.

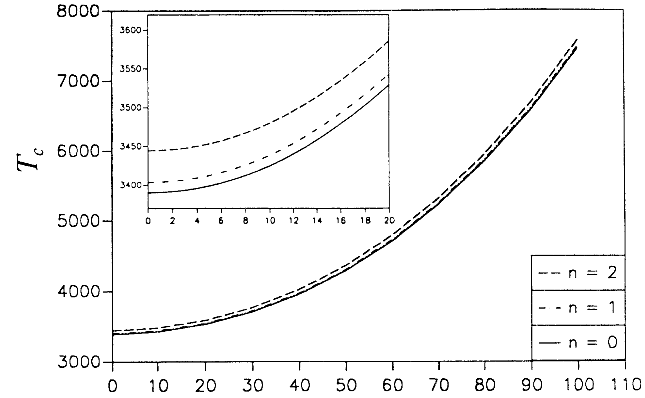

FIG. 12. The critical Taylor number as a function of the Reynolds number for different azimuthal wave numbers: $\mu=0$, $\beta=2$, and $\eta=0.95$ for $n=0$, 1 and 2.

respects, their results differ from ours and indicate that various scenarios for frequency adjustment are possible in modulated systems which are capable of giving rise (without modulation) to instabilities that have well-defined frequencies.

Although the above results have intrinsic interest, Fig. 12 indicates that special methods might have to be employed to observe them, due to the fact that axisymmetric disturbances are found to be the most unstable form of disturbances for $\beta=2$ and $\mu=0$. This result has been found to hold up to the highest value of Re used, namely Re$=100$. This is well above the value of Re at which nonaxisymmetric disturbances become unstable for a steady axial Poiseuille flow. The conclusion is that the axial oscillation stabilizes nonaxisymmetric disturbances even more than axisymmetric disturbances, which is an interesting result on its own. However, the differences between the stability curves are not great, and so the

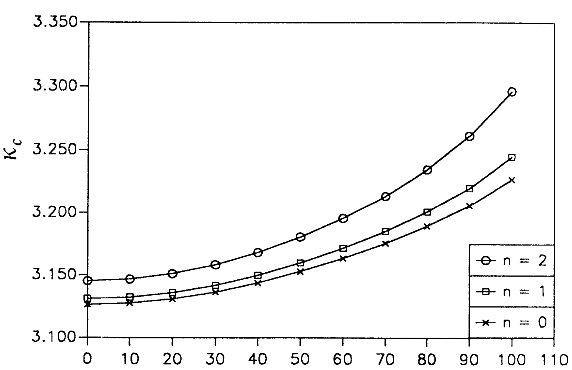

FIG. 13. The critical wave number as a function of the Reynolds number for different azimuthal wave numbers: $\mu=0$, $\beta=2$, and $\eta=0.95$ for $n=0$, 1, and 2.

effects described above for nonaxisymmetric disturbances might possibly be observed by using some means of inducing such disturbances (e.g., by altering the geometry of the inner cylinder). The critical wave numbers for the nonaxisymmetric disturbances are shown in Fig. 13 and exhibit a gradual increase with Re.

VI. SUMMARY AND CONCLUSIONS

Using linear theory, we have investigated the onset of Taylor-vortex flow when an axial motion due to a pressure gradient oscillation is imposed between the two cylinders or when the inner cylinder oscillates in the axial direction. Under the axisymmetric and the narrow-gap assumptions, we have derived a formula for the increase in the critical Taylor number T_2 from a parameter expansion and a solvability condition when Re is assumed to be small. We used a Galerkin method with orthogonal functions for finite values of Re. For both methods the ratios of $(T_c-T_{c,0})/\mathrm{Re}^2T_{c,0}$ and $T_2/T_{c,0}$ agree very well for $\mu\geq 0$, $n=0$, and Re up to 30. The results in the quasisteady state limit of a pressure gradient oscillation agree with those of a steady axial Poiseuille flow [10,11], and the results for an oscillation of the inner cylinder have the same property. We make the following conclusions.

(1) When $\mu\geq 0$ and $n=0$, the critical Taylor numbers can be predicted by use of a small amplitude analysis even for Re up to 30.

(2) For axisymmetric disturbances, we can always obtain larger critical Taylor numbers when we impose a pressure gradient oscillation between the two cylinders than when we do not. The same conclusion holds for an oscillation of the inner cylinder as long as $\mu\geq 0$. But when $\mu<0$, we find destabilization when the inner cylinder oscillates at a low value of frequency (β).

(3) The maximum stabilizing effect occurs in the quasisteady limit on the basis of this analysis when we impose a pressure gradient oscillation. But when the inner cylinder oscillates, the maximum stabilization occurs at some nonzero value of β.

(4) For $\mu=0$ and axisymmetric disturbances, the critical Taylor number increases monotonically for both oscillatory motions up to Re$\cong 100$, the largest value considered. The critical wave number decreases as Re^{-1} for the oscillation of the inner cylinder, whereas it increases slightly when a pressure gradient oscillation occurs.

(5) From the nonaxisymmetric results for $\mu=0$, we conclude that the critical Taylor number occurs for axisymmetric modes when we impose an oscillatory axial Poiseuille flow and that therefore the oscillation seems to stabilize nonaxisymmetric disturbances.

(6) The response of nonaxisymmetric modes is in general quasiperiodic, and involves one frequency that exhibits jumps as the forcing frequency and Reynolds number are changed.

The stabilization predicted in this paper cannot continue indefinitely as Re increases. Higher centrifugal modes might begin to appear, or a hydrodynamic (shear) instability will set in. The question of the maximum possible amount of stabilization will hopefully also be discussed in a later paper, as will the occurrence of nonaxisymmetric instabilities for $\mu \neq 0$.

ACKNOWLEDGMENTS

This material is based upon work supported by the NSF under Grant No. CTS-9123553. The authors wish to acknowledge the helpful comments of Professor P. Hall.

---

[1] C. W. Meyer, D. S. Cannel, and G. Ahlers, Phys. Rev. A **45**, 8583 (1992).
[2] J. Donnelly, in *Nonlinear Evolution of Spatio-Temporal Structures in Dissipative Continuous Systems,* edited by F. H. Busse and L. Kramer (Plenum, New York, 1990), p. 31.
[3] R. E. Kelly and H.-C. Hu, J. Fluid Mech. **249**, 373 (1993).
[4] R. E. Kelly and H.-C. Hu, Heat Transfer **7**, 79 (1994).
[5] C. F. Barenghi and C. A. Jones, J. Fluid Mech. **208**, 127 (1989).
[6] H. Kuhlmann, D. Roth, and M. Lücke, Phys. Rev. A **39**, 745 (1989).
[7] P. Hall, J. Fluid Mech. **67**, 29 (1975).
[8] P. J. Riley and R. L. Laurence, J. Fluid Mech. **75**, 625 (1976).
[9] S. Chandrasekhar, *Hydrodynamic and Hydromagnetic Stability* (Dover, New York, 1981).
[10] E. R. Krueger and R. C. DiPrima, J. Fluid Mech. **19**, 528 (1964).
[11] R. C. DiPrima and A. Pridor, Proc. R. Soc. London Ser. A **366**, 555 (1979).
[12] K. C. Chung and K. N. Astill, J. Fluid Mech. **81**, 641 (1977).
[13] D. I. Takeuchi and D. F. Jankowski, J. Fluid Mech. **102**, 101 (1981).
[14] B. S. Ng and E. R. Turner, Proc. R. Soc. London Ser. A **382**, 83 (1982).
[15] K. L. Babcock, G. Ahlers, and D. S. Cannell, Phys. Rev. Lett. **67**, 3388 (1991).
[16] K. Bühler and N. Polifke, in *Nonlinear Evolution of Spatio-Temporal Structures in Dissipative Continuous Systems* (Ref. [2]), p. 21.
[17] R. M. Lueptow, A. Docter, and K. Min, Phys. Fluids A **4**, 2446 (1992).
[18] E. R. Krueger, A. Gross, and R. C. DiPrima, J. Fluid Mech. **24**, 521 (1966).
[19] P. H. Roberts, J. Math. Anal. Appl. **1**, 195 (1960).
[20] S. Chandrasekhar, J. Math. Mech. **10**, 683 (1961).
[21] C. W. Gear, *Numerical Initial Value Problems in Ordinary Differential Equations* (Prentice-Hall, New York, 1971).
[22] D. L. Harris and W. H. Reid, Astrophys. J. Suppl. Ser. **3**, 429 (1958).
[23] E. A. Coddington and N. Levinson, *Theory of Ordinary Differential Equations* (McGraw-Hill, New York, 1955).
[24] F. H. Busse, Z. Angew. Math. Mech. **50**, 173 (1970).
[25] P. Hall, J. Fluid Mech. (to be published).
[26] S. K. Datta, J. Fluid Mech. **21**, 635 (1965).
[27] C.-M. Ho and L.-S. Huang, J. Fluid Mech. **119**, 443 (1982).